Temporal and spatial distribution of gentamicin in the peripheral vestibular system after transtympanic administration in guinea pigs

Ru Zhang[a,1], **Yi-Bo Zhang**[a,1], **Chun-Fu Dai**[a,*], and **Peter S. Steyger**[b]

[a]Department of Otology and Skull Base Surgery, Eye Ear Nose and Throat Hospital, Fudan University, 83 Fen Yang Road, Shanghai 200031, China

[b]Oregon Hearing Research Center, Oregon Health & Science University, Portland, OR 97239, USA

Abstract

Background and objective—Transtympanic administration of gentamicin is effective for treating patients with intractable vertigo. This study explored the spatial and temporal distribution of gentamicin in vestibular end-organs after transtympanic administration.

Methods—Thirty guinea pigs were transtympanically injected with gentamicin conjugated to Texas Red (GTTR) and their vestibular end-organs examined after various survival periods. Another 9 guinea pigs received GTTR at different doses. Nine animals received Texas Red only and served as controls. We used confocal microscopy to determine the cellular distribution of GTTR in semicircular canal cristae, as well as the utricular and saccular maculae.

Results—The most intense GTTR labeling was present in the saccule compared to other vestibular end-organs. GTTR fluorescence was detected predominantly in type I hair cells, type II hair cells and transitional cells after a single transtympanic dose of GTTR (0.1 mg/ml, 0.05 ml), while only weak fluorescence was observed in non-sensory cells such as supporting cells, dark cells and lumenal epithelial cells. Transitional cells displayed intense GTTR fluorescence in the supra-nuclear regions 24 h after transtympanic injection that was retained for at least 4 weeks. A decreasing spatial gradient of GTTR fluorescence was observed sensory epithelial regions containing central type I to peripheral type I and then type II hair cells in the crista ampullaris, and from striolar to extra-striolar hair cells within the vestibular macula. GTTR fluorescence extended from being restricted to the apical cytoplasm at lower doses to the entire cell body of type I hair cells with increasing dose. GTTR fluorescence reached peak intensities for individual regions of interest within the cristae and maculae between 3 and 7 days after transtympanic injection.

Conclusion—The saccular uptake of GTTR is greater than other vestibular end-organs after transtympanic injection in the semicircular canals.

1. Introduction

Transtympanic administration of aminoglycosides has been considered an effective and economical approach for clinical treatment of intractable Meniere's disease since its first demonstration by Schuknecht when streptomycin was injected transtympanically (1956). A meta-analysis indicated that complete vertigo control (class A) was achieved in 74.7% of

[*]Corresponding author. Tel.: +86 21 64377134; fax: +86 21 64377151. cfdai66@yahoo.com.cn (C.-F. Dai).
[1]Both the authors made equal contributions to this work.

patients and complete or substantial (class B) control of vertigo was obtained in 92.7% of patients after transtympanic administration of gentamicin (Cohen-Kerem et al., 2004). However, the precise mechanism underlying gentamicin control of vertigo and the optimal dose of gentamicin to treat Meniere's disease remains unclear. Studies showed that gentamicin-induced toxicity of vestibular sensory hair cells partially ablated vestibular function, and represents one mechanism of vertigo control (Hirvonen et al., 2005). Following transtympanic injection, gentamicin generally diffuses through the round window membrane into cochlear perilymph and is subsequently taken up by vestibular hair cells (Becvarovski et al., 2002). More recent studies have demonstrated that drug may enter the inner ear through both the round and oval windows in both experimental animals and humans studies (Salt et al., 2012; King et al., 2011).

Lopez et al. described severe damage of vestibular hair cells 7 days after transtympanic administration of gentamicin, with initial signs of hair cell recovery at 28 days post-injection in chinchillas (Lopez et al., 1997). Hirvonen et al. (2005) reported that head tilt reached its maximum in chinchillas 5–25 days after transtympanic injection of gentamicin and that hair cell damage present for at least 3 weeks. In the cochlea, the greatest uptake of gentamicin occurred in cochlear outer hair cells at 3 days and was retained for at least 3 weeks following transtympanic injection (Zhai et al., 2010). Despite numerous studies emphasizing the functional changes of inner ear and associated pathology following transtympanic injection of gentamicin, the temporal and spatial distribution of gentamicin and correlation with vestibulotoxicity remains to be elucidated.

The function of individual vestibular end-organs can be evaluated using the caloric test (low frequency, horizontal semicircular canal), head thrust test (high frequency, three semicircular canals), rotation test (horizontal semicircular canal), dynamic visual acuity (three semicircular canals), cervical vestibular evoked myogenic potential testing (cVEMP; saccule) and ocular vestibular evoked myogenic potential testing (oVEMP; utricule) (Curthoys et al., 2009). De Waele et al. (2002) postulated that the saccule was more sensitive than the horizontal semicircular ampullaris to the ototoxic effects of transtympanic gentamicin based on their results of caloric test, head thrust test and VEMP tests on patients with intractable Meniere's disease. Helling et al. reported that transtympanic application of gentamicin effectively eliminates semicircular canal and saccular function, but exerts less effect on utricular function in patients with unilateral Meniere's disease (Helling et al., 2007). However, it remains unclear why the utricle should be less susceptible to gentamicin than other end-organs.

Transtympanic application of gentamicin caused greater loss of type I hair cells than type II hair cells, which is attributed to the preferential uptake of the drug by type I hair cells than the type II hair cells and supporting cells after administration (Lopez et al., 1997; Imamura and Adams, 2003; Hirvonen et al., 2005; Lyford-Pike et al., 2007; Roehm et al., 2007). Additionally, the central zone of semicircular canal ampullae and the striola of the utricular and saccular maculae are more susceptible than peripheral sensory epithelia (Lyford-Pike et al., 2007). Based on these studies, we hypothesized that a gradient of gentamicin uptake from central type I hair cells to peripheral type I and type II hair cells after transtympanic administration.

Pender (1985) reported acute damage to the basal infoldings of dark cells at one month that persisted for at least six months after transtympanic administration of gentamicin in cats. This suggests that transtympanic application of gentamicin may also relieve endolymphatic hydrops by disrupting dark cell regulation of endolymph (Pender,1985). However, human temporal bone studies revealed no decrease of dark cell number within 6 months after a parenteral administration of aminoglycosides (Cureoglu et al., 2003). More recent study

using MRI demonstrated that intratympanic gentamicin injection fails to reduce endolymphatic hydrops in patients with Meniere's disease (Fiorino et al., 2012). Dark cells regulate the composition of vestibular endolymph, and Na^+/K^+-adenosine triphosphatase activity was retained on the basolateral membranes of dark cells after transtympanic administration in guinea pigs (Yoshihara et al., 1994). Recent studies have reported dark cell uptake of gentamicin after transtympanic administration (Roehm et al., 2007), and another study demonstrated immunolocalized gentamicin at the apex of transitional cells (Imamura and Adams, 2003).

In this study, we used gentamicin conjugated to Texas Red (GTTR) as a tracer to explore the temporal and spatial distribution of gentamicin in various vestibular end-organs and cell types. We also immunolabeled tissues for calretinin as the marker of type I hair cells located within the central region of cristae and striola of maculae (Leonard and Kevetter, 2002) to differentiate the uptake of GTTR within different regions of vestibular organ.

2. Materials and methods

2.1. Animals

Adult male or female albino guinea pigs weighing 250–300 g were used in this study. Thirty animals received 50 µl of purified GTTR (0.1 mg/ml) by transtympanic injection and were sacrificed at 1, 3, 7,14, 28 days (for transverse sections) and 7 days (for whole-mounts; 5 guinea pigs per group). An additional 9 guinea pigs (3 in each group) received different doses (0.1, 0.4 or 0.8 mg/ml) of GTTR and were sacrificed at 7 days later. Another 9 guinea pigs (3 in each group) served as controls, and received various equivalent 50 µl doses of Texas Red (TR) only (0.065, 0.205 or 0.510 mg/ml). The left ear was treated in all animals. All experimental protocols were performed in accordance with the guidelines of Ethical Board of Eye Ear Nose and Throat Hospital, Fudan University (Shanghai), and approved by the Institutional Committee on Care and Use of Animals.

2.2. Conjugation and purification of GTTR

An excess of gentamicin (in K_2CO_3, pH 10) was mixed with Texas Red (TR) stock solution for conjugation and then was separated by reversed phase chromatography to purify the conjugated GTTR from unconjugated gentamicin and potential contamination by unreacted TR (Myrdal et al., 2005). The isolated GTTR conjugate was aliquoted, lyophilized, and stored desiccated, in the dark at −20 °C until required. Purified GTTR and TR was reconstituted as 1.0 mg/ml stock solution with 25 µl DMSO in each vial stored at −20 °C protected from light. The stock GTTR (or TR) solution was diluted for injection with sterile phosphate buffered saline (PBS, pH 7.4).

2.3. Gentamicin administration and tissue collection

Guinea pigs, without visible otitis media, were anesthetized using intramuscular ketamine (40 mg/kg) and xylazine (10 mg/kg). The external auditory canal was sterilized with 75% ethanol solution. GTTR (50 µl) solution was injected into the tympanic cavity after puncturing the tympanic membrane using a 100 µl microsyringe. The head was held stationary with the treated ear and nose turned toward the ceiling so as to bathe the round window niche in solution for 30 min. For the control groups, TR solution was administered in the same manner. At each timepoint, guinea pigs were deeply anesthetized, prior to sequentially excising the left temporal bone, rapidly opening the bulla, removing the stapes and round window, performing a cochleostomy at the cochlear apex, and perfusing the inner ears with 4% paraformaldehyde via round and oval windows; the entire inner ear was then immersed in the same fixative solution overnight at 4 °C. The vestibular end-organs were harvested in PBS. For transverse sections, we processed excised tissues through graded

sucrose solutions (20%, 30%), and embedded them in Tissue Tek OCT compound prior to rapid cooling with dry ice for 5 min, and transverse sectioning (10 μm) using a cryostat (Leica, Germany). Four sections close to the midline of each organ were selected for immunofluorescence.

2.4. Immunofluorescence and confocal microscopy

After washing in 0.01 M PBS (pH = 7.2–7.4; 3×10 min), sections were immunoblocked with 10% goat serum in 0.2% Triton X-100 for 1 h at room temperature (20–25 °C) to reduce non-specific immunoreactivity, incubated in mouse anti-calretinin monoclonal antibodies (1:250; Millipore) diluted in immunoblocking solution for 24 h at 4 °C, and secondarily-labeled with Alexa Fluor-488-conjugated goat anti-mouse antibodies (1:200 in PBS containing 5% goat serum and 0.1% Triton X-100, Invitrogen, CA) for 2 hat room temperature. Subsequently, sections were incubated with 4,6-diamidino-2-phenylindole (DAPI, 1:500 in PBS; Invitrogen) for 20 min at room temperature to label nuclei. Between all labeling steps, 3×10-min rinses in PBS were performed. Sections were then mounted under coverslips on glass slides in a 1:1 mixture of 0.1 M PB and glycerol. The same protocol was also applied to the whole mount tissues except for transferring to slides after immunolabeling. Control tissues were processed with the same protocol except using PBS to replace the primary antibody. All incubation steps were done in the dark.

Sections from the midportion of each end-organ were scanned using a confocal laser scanning microscopy (TCS SP5, Leica, Germany). Eight serial optical slices (at 1.0 μm steps) through the sections were obtained with the identical parameters (laser power, gain and pinhole). Whole mount specimens were scanned from the surface 10 μm into the tissue to obtain 10 serial optical sections (1.0 μm step-size) in the same manner. Amplifier offset and detector gain were optimized for each end-organ to prevent saturation of pixels in the images, and sequentially for each laser setting. Confocal imaging of control sensory epithelia was performed at the same laser intensity and gain settings used for sensory epithelia from GTTR-treated guinea pigs. The intensity of GTTR fluorescence within the cells of vestibular sensory epithelia was quantified using the image analysis software Image Pro-Plus 6.0. The intensity of GTTR fluorescence was measured with a grayscale value (0–255, arbitrary fluorescent units, AFU). All images were prepared for publication using Photoshop.

Texas Red (the fluorophore in GTTR) is extremely stable in visible light and does not photobleach or quench rapidly (Brismar et al., 1995; Liu et al., 2005). Fluorescent intensity analyses were performed on GTTR fluorescence before and after 1, 2 and 4 h exposure to incandescent light equivalent to processing and exposure to light during sectioning. Total fluorescence was obtained from histogram data for each image and summing the products of intensity and frequency. All sums were within 10% of the overall mean, without any statistically significant difference (data not shown). Thus, there was no evidence of photobleaching of GTTR during processing and sectioning of fluorescently-labeled tissues.

2.5. GTTR intensity measurements and cell identification

As reported previously, type I hair cells were identified by their flask shape with constricted necks within the epithelia, as well by the calretinin immunolabeled calyx within the central zone of the crista ampullaris and striola of the maculae. Type II hair cells were identified by a more apically located nucleus, their cylindrical morphology and lack of calretinin immunolabeled calyces (Lyford-Pike et al., 2007). The supporting cells were identified by their dense heterochromatin and nuclear location adjacent to the basal lamina (Lysakowski and Goldberg, 2004). Dark cells were identified by their characteristic irregular morphology and relative location with the peripheral zone of cristae, and transitional cells by their

columnar morphology within a shallow concave crypt between the sensory epithelia of cristae and surrounding dark cells. The operator outlined the borders of cells so that the intensity measured included the cytoplasm and nucleus. This was facilitated by scrolling through the optical slices of the z-stack and selecting the different laser channels. The central zone of the cristae and striola of the maculae were approximately 50×100 μm according calretinin-positive immunofluorescence.

2.6. Statistics

General linear model (GLM) analyses of variance were performed on these data to determine any statistically significant difference between treatments, animal groups, end-organs, and cell types. Variables identified as significantly different were then further analyzed via post-hoc ANOVA and t tests.

3. Results

3.1. Saccular uptake of GTTR is greater than other vestibular end-organs after transtympanic injection

GTTR fluorescence was detected in the 3 ampullae and 2 maculae 7 days after transtympanic injection (0.1 mg/ml, 0.05 ml; Fig. 1). Animals treated with the equivalent dose of unconjugated TR (0.1 mg/ml, 0.05 ml, 7 days) did not reveal any non-specific fluorescence (not shown). Single fluorophore images revealed visible GTTR fluorescence in transverse sections (Fig. 1A–E) and whole-mounted vestibular end-organs (Fig. 1F–J) and showed more intense fluorescence in the saccule (E and J) compared to other organs (A–D and F–I) at this timepoint, 7 days. In sections, GTTR fluorescence was bright at the level of the sensory hair cells, negligible within the zone occupied by supporting cell bodies, and diffusely distributed through the interstitial zone beneath the sensory epithelium (Fig. 1A–E). In sections of cristae, transitional cells, within a concave crypt at the base of the cristae ampullarae, displayed more intense fluorescence compared to hair cells in the same crista (Fig. 1A–C; see below).

Calretinin, a protein mainly detected in calyx of central or striolar-associated type I hair cell (Fig. 1, F1–JI), is a specific marker of central type I hair cell of cristae, or striolar type I hair cell of maculae. DAPI labels the ds-DNA in the nuclei of all cell types. We used calretinin and DAPI to differentiate the central hair cells from others. Transverse images of triple-labeled sections showed calretinin-positive type I hair cells mainly within the central zone of cristae (Fig. 1, A1–C1) and striola of maculae (Fig. 1, D1 and E1). In whole-mounted cristae (Fig. 1, F–H, F1–H1), we can only see the calretinin-positive central zone with GTTR fluorescence due to its elevated surface. In the maculae, the striola is clearly identified with caretinin-positive labeling (Fig. 1, I1 and J1).

Quantitative intensity analysis of sections revealed that the saccule had greater GTTR fluorescence than the utricle ($P < 0.05$) or semicircular canal cristae ($P < 0.001$; Fig. 2). In addition, the intensity of GTTR in the posterior crista is greater than that in the superior and horizontal cristae ($P < 0.05$; Fig. 2A). We also measured the intensity of GTTR fluorescence in the central zone of cristae and striolae of maculae in whole-mounts (Fig. 2B). These data revealed that saccular striolar hair cells take up more GTTR than type 1 hair cells of other end-organs ($P < 0.001$), and no significant difference in GTTR fluorescence was present among type I hair cells of the 3 cristae and the utricule.

3.2. Cellular distribution of GTTR fluorescence in semicircular canal cristae

GTTR fluorescence was detected predominantly in type I hair cells, type II hair cells and transitional cells 7 days (Fig. 3) after a single transtympanic injection of GTTR (0.1 mg/ml,

0.05 ml), while only weak fluorescence was observed in non-sensory cells such as supporting cells, dark cells (Fig. 3D1) and lumenal epithelial cells (Fig. 3D2) at this timepoint. Ampullar type I and II hair cells of central (Fig. 3E1) and peripheral zones (Fig. 3E2)of the crista showed intense GTTR fluorescence largely localized within the apical cytoplasm, with positive calretinin labeling the neural calyx surrounding central type I hair cells (Fig. 3E1). The supporting cell bodies are largely located beneath the hair cells and exhibited little GTTR fluorescence (Fig. 3E2). Transitional cells displayed intense GTTR fluorescence 7 days after transtympanic injection, particularly in their apical cytoplasm (Fig. 3E3), and was retained for at least 28 days (not shown).

3.3. Gradient intensity of GTTR fluorescence within the vestibular sensory epithelium

When different doses of GTTR were injected transtympanically (0.1, 0.4, 0.8 mg/ml), GTTR fluorescence extended from the apical cytoplasm to fill the whole cell body in type I hair cells with increasing dose (Fig. 4). We measured GTTR fluorescence intensity in the different cell types at 0.1, 0.4 and 0.8 mg/ml doses respectively. A decreasing gradient of GTTR fluorescence was revealed in ampullar sensory epithelial regions containing central type I (calretinin-positive) to peripheral type I (calretinin-negative) and type II hair cells at the highest dose of GTTR. There were statistically significant differences between central type I hair cells and peripheral type I hair cells or type II hair cells ($P< 0.001$, Fig. 5). Transitional cells displayed greater GTTR fluorescence than the sensory epithelial cells in the 0.1 mg/ml group (Fig. 5A, $P< 0.001$), and comparatively less intense GTTR fluorescence than sensory hair cells in the 0.8 mg/ml group (Fig. 5B, $P< 0.001$), and showed no statistically significant difference of fluorescence intensity between the 0.1 and 0.8mg/ml group, which indicated the transitional cells may be rapidly saturated by GTTR uptake, even at lower doses of GTTR.

3.4. Temporal distribution of GTTR in the peripheral vestibular system

To explore the temporal distribution of GTTR in the peripheral vestibular system, we analyzed the intensity of GTTR fluorescence in each end-organ (utricle, saccule and the three ampullae) at 1, 3, 7, 14 and 28 days after transtympanic injection. Guinea pigs injected with TR only displayed negligible fluorescence at 1 or 7 days after injection (Fig. 6A1–C1). Cryostat-sectioned tissues from guinea pigs transtympanically injected with 0.1 mg/ml GTTR had GTTR fluorescence in all vestibular epithelia after 24 h (Fig. 6A2–C2) and intense fluorescence at 7 days (Fig. 6A3–C3). Statistical analysis revealed that the intensity of GTTR fluorescence peaked between 3 and 14 days, likely ~day 7, and had decreased significantly by 28 days ($P< 0.05$, Fig. 7) for all maculae and ampullae respectively. Comparisons of GTTR intensity between 1 day and 7 days and between 7 days and 28 days for each kind of organ showed statistical differences ($P< 0.05$, Fig. 7).

4. Discussion

In this study, we transtympanically injected GTTR to explore the distribution of gentamicin in each vestibular organ and demonstrated that GTTR reached the peak intensity around 7 days after local administration. A decreasing concentration gradient of GTTR uptake was observed from central to peripheral type I and then to type II hair cells within the sensory epithelia of the crista ampullarae, and from striolar to extra-striolar hair cells in the maculae. Within the hair cell, GTTR was primarily deposited in the apical cytoplasm and then extended throughout the cytoplasm with increasing dose. In addition, transitional cells displayed GTTR fluorescence in the supra-nuclear regions at 24-h post-injection, when the first time-point we examined, and was retained for up to 4 weeks. Other cells took up GTTR, including dark cells, epithelial cells in the planum semilunare, and within the stroma

below the sensory epithelia. Furthermore, the saccule took up more GTTR than the utricle and ampulla, with comparatively less GTTR fluorescence in dark cells.

4.1. Saccular uptake of GTTR is greater than the utricle and ampullae after transtympanic injection

Kuo et al. (2005) studied patients with Meniere's disease during their vertigo attacks and documented that 8 of 12 (67%) subjects had abnormal VEMPs, indicating that the saccule was involved in the vertigo attack. Manzari et al. (2010) reported that a patient presenting with subjective vertigo, nausea and vomiting was shown to have a purely saccular lesion, which further support the saccule as a source of vertigo. Day et al. (2007) reported that the saccule was significantly damaged 7 days post-transtympanic gentamicin injection in guinea pigs, and confirmed that the absence of cervical click-evoked myogenic potentials can be attributed to lesions in the saccule. Other studies have shown that the saccule takes up gentamicin or GTTR after systemic administration in bullfrogs (Dai et al., 2006) or guinea pigs (Imamura and Adams, 2003). Transtympanic injection of gen-tamicin appears to preferentially affect saccular function compared utricular or semicircular canal function (Helling et al., 2007; De Waele et al., 2002). However, it is not known whether the distinct toxic effects of gentamicin in the different vestibular organs were due to different degrees of gentamicin uptake, i.e. leading to variable levels of toxicity in hair cells in different epithelia, or due to greater sensitivity of saccular hair cells to gentamicin.

We used GTTR as a tracer for gentamicin to explore drug uptake in the five vestibular end-organs in guinea pigs. Both transverse sections of, and whole-mounted, tissues were used to measure GTTR fluorescence intensity after transtympanic injection, which revealed greater GTTR uptake by the saccule compared to the semicircular canal cristae or the utricule. This indicates that the decreased effect of gentamicin-induced toxicity on utricular and ampullar function compared to the saccule may be due to reduced drug uptake compared to the saccule, although we cannot exclude the possibility that saccular hair cells are more sensitive to the gentamicin-induced cytotoxicity. These data also show that saccule may be the primary target following transtympanic gentamicin injection and that cervical VEMP testing could be used as an early indicator of gentamicin-induced vestibular dysfunction. Vertigo attacks do not recur in patients when the gVEMP (VEMP evoked by short duration galvanic currents) was abolished. Therefore, gVEMPs may also predict treatment outcomes and serve as the end-point of treatment (De Waele et al., 2002).

The comparatively more intense GTTR fluorescence in the saccule is likely associated with the relative locations of the 5 vestibular end-organs, and the inner ear trafficking route of gentamicin after transtympanic injection. Of the 5 vestibular end-organs, the saccule is closest to the cochlear oval and round windows. Although previous studies reported drug entry from the middle ear into perilymph occurs primarily via the round window (Plontke et al., 2007), more recent studies emphasize that drugs may also enter the inner ear through the oval window, providing more direct access to the vestibule (King et al., 2011; Salt et al., 2012). The vestibular system appears to act as a "sink" and the highest levels of transtympanic gadolinium were observed in the vestibule compared to the cochlea (King et al., 2011).

4.2. GTTR levels in different cell types

Previous studies have reported that the central region of the crista was most severely damaged following transtympanic administration of aminoglycosides, compared to the periphery of the crista, or the region close to the planum semilunatum lateral to the cristae (Lindeman, 1969; Wersall et al., 1971; Ikeda and Morgenstern, 1992). Type I hair cells were more severely damaged than type II hair cells (Wersall et al., 1971; Lopez et al., 1997;

Hirvonen et al., 2005). Hayashida et al. (1985) and Lyford-Pike et al. (2007) reported that gentamicin was initially localized in type I hair cells after systemic or local gentamicin administration, suggesting that the degree of damage was associated with drug uptake. This study revealed that calretinin-positive centrally-located type I hair cells had comparatively more GTTR than calretinin-negative, peripheral type I hair cells or type II hair cells, potentially correlating with similar regional differences in vulnerability to ototoxic antibiotics.

Gentamicin can enter hair cells through the mechanoelectrical transduction channels at the tips of stereocilia (Marcotti et al., 2005) or via apical endocytosis (Hashino and Shero, 1995). The different bundle structures of type I hair cells compared to type II hair cells may explain the greater uptake of gentamicin by type I hair cells. Type I hair bundles are taller and contain more stereocilia with larger diameter than type II hair bundles (Xue and Peterson, 2006). Each stereocilium contains one or two aminoglycosidepermeant transduction channels, and the greater number of stereocilia on the type I hair cells, with larger transduction current amplitudes (Lysakowski and Goldberg, 2004), could also facilitate greater uptake of gentamicin than in Type II hair cells. Secondly, the electrochemical driving force may also be involved. Chen and Eatock reported that isolated rat type I hair cells in the cristae have more negative resting potentials than the type II hair cells (Chen and Eatock, 2000), which may also lead to a greater electrochemical driving force for cationic gentamicin to enter type I hair cells compared to type II hair cells. The more intense GTTR labeling of type I hair bundles appears to correlate with this interpretation.

4.3. Cellular distribution of GTTR within vestibular epithelium

A recent study reported that gentamicin immunolabeling and GTTR fluorescence were primarily localized at the apical region of type I hair cells after a single transtympanic injection in chinchillas (Lyford-Pike et al., 2007). In this study, we also observed GTTR initially in the apical cytoplasm of type I hair cells, with weaker, diffuse fluorescence throughout the cell. With increasing GTTR dose, greater GTTR fluorescence was observed in the perinuclear cytoplasm but still weaker than at the apical region. Type II hair cells showed the similar labeling pattern, however, the labeling in type II hair cell was less intense than that in the type I hair cells. This differential distribution pattern may be associated to the degree of drug entry into hair cells as described above. At lower doses, GTTR entering hair cells through the stereociliary transduction channels may be sequestered in the apical cytoplasm by gentamicin binding proteins (Karasawa et al., 2010, 2011). With increasing dose, the drug may saturate these binding proteins and is then present diffusely throughout the cytosol. Wang and Steyger (2009) demonstrated that the cochlear distribution of gentamicin-Texas Red (GTTR) is closely correlated to the cochlear distribution of immunolabeled or tritiated gentamicin, despite the slower serum pharmacokinetics of GTTR due to its larger molecular size. In addition, they also demonstrated that increasing dose of GTTR is correlated with increasing cellular fluorescence. In addition, endocytosis of GTTR could be transported to Golgi bodies, endoplasmic reticuli and lysosomes that are mainly situated in the apical cytoplasm of hair cells (Hashino and Shero, 1995; Steyger et al., 2003; Sandoval et al., 1998, 2000). It has been hypothesized that intracellular membranes encapsulating aminoglycosides could subsequently rupture and release the drug into the cytoplasm, leading to proteolytic cell death (Hashino et al., 1997).

4.4. Time course of GTTR distribution in the vestibular epithelium

Lopez et al. (1997) reported that the greatest degree of vestibular degenerative changes occurred 7 days following transtympanic gentamicin application, and initial signs of hair cell recovery appeared at 28 days. Hirvonen et al. (2005) observed that head tilt appeared to

reach its maximum in animals between 5 and 25 days after transtympanic injection and the hair cell degeneration lasted at least three weeks. Zhai et al. (2010) showed intense GTTR fluorescence in cochlear outer hair cells within 3 days that was retained for at least 3 weeks. In this study, we observed that the intensity of GTTR fluorescence in vestibular epithelia peaked about 7 days after a single transtympanic injection. The larger molecular weight of GTTR (Wang and Steyger, 2009) may slow the bulk trafficking of GTTR compared to native gentamicin that entry of GTTR into vestibular cells continues over a longer period of time compared to gentamicin. We can conclude that the time course of hair cell dysfunction and subsequent degeneration is closely correlated with the temporal uptake of gentamicin.

To the best of our knowledge, several previous studies (Roehm et al., 2007; Lyford-Pike, S. et al., 2007; Imamura and Adams, 2003) have demonstrated that gentamicin is retained in hair cells for up to six months. The density of gentamicin labeling in inner ear tissues changed over time, and is corroborated in our studies here using GTTR. We routinely use 26.7 mg/ml gentamicin clinically for patients with Meniere's disease. However, intratympanic gentamicin doses of 26.7 mg/ml (or more, as used in Imamura and Adams, 2003) cause severe damage to vestibular hair cells in guinea pigs, with consequent disruption of drug distribution analysis. Thus, in this study, we used 0.1 mg/ml GTTR as a tracer to explore the distribution of gentamicin in the vestibular system. The rationale for choosing 4 weeks as the longest timepoint was based on the study by Hirvonen et al. (2005), who reported that head tilt reached its maximum in chinchillas 5–25 days after transtympanic injection of gentamicin and that hair cell damage occurred within 4 weeks. GTTR was still retained by all sensory epithelia at 4 weeks after transtympanic injection in this study. Furthermore, we have previously shown clinically that a single intratympanic gentamicin injection, and patient follow-up 3 weeks later, was optimal to determine the end-point of gentamicin therapy (Zhai et al., 2010).

4.5. Uptake of GTTR by non-sensory cells: dark cells

Park and Cohen (1982) reported that streptomycin damaged the dark cells before affecting other cells, suggesting that the primary target of streptomycin was the ion-regulating tissues of the vestibule and that the loss of vestibular hair cells was due to a disturbance of the microhomeostasis of vestibular endolymph. Ge and Shea (1993, 1995) reported that the dark cells in the membranous wall of the utricle were also affected by streptomycin, indicating that streptomycin may cause dysfunction of utricular dark cells, reducing the volume of utricular endolymph. Roehm et al. (2007) reported gentamicin uptake by dark cells using both gentamicin immunohistochemistry and tritiated gentamicin. In contrast, dark cells retained Na^+/K^+-adenosine triphosphatase activity on their folded basolateral membranes after a 5- or 15-day period of parenteral gentamicin treatment, suggestive of continued ion regulation of endolymph (Yoshihara et al., 1994). Furthermore, human temporal bones demonstrated less dark cells loss following a short period of gentamicin treatment (Cureoglu et al., 2003). In this study, after transtympanic injection of GTTR, comparatively weak GTTR uptake was observed in dark cells compared to other cell types (Fig. 3D1). It suggests that dark cells are not the primary target in the peripheral vestibule after intratympanic gentamicin injection for the management of patients with intractable vertigo. It is consistent with recent study that intratympanic gentamicin injection fails to reduce endolymphatic hydrops in patients with Meniere disease (Fiorino et al., 2012).

4.6. Transitional cells

The transitional cells are located in a concave crypt between the hair cells and dark cells in the crista ampullaris. They appear to provide a simple barrier to sustain the high concentration differences of K^+ and Na^+ between endolymph and perilymph and actively absorb cations by cellular mechanisms homologous to cochlear outer sulcus cells (Oudar et

al., 1988; Lee et al., 2001). Previous studies revealed that KCNE1 channels, TREK-1, ephrin-B2, Na/H exchanger and P2×2 receptor et al. are expressed in the transitional cells and are related to the K^+ recycling (Bartolami et al., 2011; Nicolas et al., 2004; Dravis et al., 2007; Lee et al., 2001). In this study, we observed intense, punctate GTTR fluorescence in the apical region of transitional cell 7 days after transtympanic injection that retained for at least 28 days. We also observed that GTTR fluorescence in transitional cells was not increased with the increasing GTTR doses, suggestive of rapid cellular saturation with the drug. However, it is still unknown why transitional cells have such rapid and distinctive GTTR uptake, or whether there is any ototoxic effect on these cells. Transitional cells may act as a pathway for GTTR trafficking from vestibular perilymph into endolymph, or alternatively, sequester GTTR from vestibular endolymph.

5. Conclusion

Based on the above data, we propose that the saccule may be the primary target following transtympanic gentamicin injection and that cervical VEMP testing could be used as an early indicator of gentamicin-induced vestibular dysfunction. Type I hair cells in the semicircular canals, rather than the dark cells, are also a primary target when transtympanic gentamicin injection is used to clinically manage intractable Meniere disease. The time course of hair cell dysfunction and subsequent degeneration appears to be closely correlated with the temporal uptake of gentamicin. Transitional cells may act as a pathway for GTTR trafficking from vestibular perilymph into endolymph, or alternatively, sequester GTTR from vestibular endolymph.

Acknowledgments

References

Bartolami S, Gaboyard S, Quentin J, Travo C, Cavalier M, Barhanin J, Chabbert C. Critical roles of transitional cells and Na/K-ATPase in the formation of vestibular endolymph. J. Neurosci. 2011; 31:16541–16549. [PubMed: 22090480]

Becvarovski Z, Bojrab DI, Michaelides EM, Kartush JM, Zappia JJ, LaRouere MJ. Round window gentamicin absorption: an in vivo human model. Laryngoscope. 2002; 112:1610–1613. [PubMed: 12352673]

Brismar H, Trepte O, Ulfhake B. Spectra and fluorescence lifetimes of lissamine rhodamine, tetramethylrhodamine isothiocyanate, texas red, and cyanine 3.18 fluorophores: influences of some environmental factors recorded with a confocal laser scanning microscope. J. Histochem. Cytochem. 1995; 43:699–707. [PubMed: 7608524]

Chen JW, Eatock RA. Major potassium conductance in type I hair cells from rat semicircular canals: characterization and modulation by nitric oxide. J. Neurophysiol. 2000; 84:139–151. [PubMed: 10899192]

Cohen-Kerem R, Kisilevsky V, Einarson TR, Kozer E, Koren G, Rutka JA. Intratympanic gentamicin for Meniere's disease: a meta-analysis. Laryngoscope. 2004; 114:2085–2091. [PubMed: 15564826]

Cureoglu S, Schachern PA, Paparella MM. Effect of parenteral aminoglycoside administration on dark cells in the crista ampullaris. Arch. Otolaryngol. Head Neck Surg. 2003; 129:626–628. [PubMed: 12810465]

Curthoys IS, Manzari L, Smulders YE, Burgess AM. A review of the scientific basis and practical application of a new test of utricular function - ocular vestibular-evoked myogenic potentials to bone-conducted vibration. Acta Otorhinolaryngol. Ital. 2009; 29:179–186. [PubMed: 20161874]

Dai CF, Mangiardi D, Cotanche DA, Steyger PS. Uptake of fluorescent gentamicin by vertebrate sensory cells in vivo. Hear. Res. 2006; 213:64–78. [PubMed: 16466873]

Day AS, Lue JH, Yang TH, Young YH. Effect of intratympanic application of aminoglycosides on click-evoked myogenic potentials in Guinea pigs. Ear Hear. 2007; 28:18–25. [PubMed: 17204896]

De Waele C, Meguenni R, Freyss G, Zamith F, Bellalimat N, Vidal PP, Tran BHP. Intratympanic gentamicin injections for Meniere disease: vestibular hair cell impairment and regeneration. Neurology. 2002; 59:1442–1444. [PubMed: 12427902]

Dravis C, Wu T, Chumley MJ, Yokoyama N, Wei S, Wu DK, Marcus DC, Henkemeyer M. EphB2 and ephrin-B2 regulate the ionic homeostasis of vestibular endolymph. Hear. Res. 2007; 223:93–104. [PubMed: 17158005]

Fiorino F, Pizzini FB, Barbieri F, Beltramello A. Magnetic resonance imaging fails to show evidence of reduced endolymphatic hydrops in gentamicin treatment of Meniere's disease. Otol. Neurotol. 2012; 33:629–633. [PubMed: 22314924]

Ge X, Shea JJ. Intramuscular streptomycin effect on dark cells of utricle in guinea pigs. Am. J. Otol. 1993; 14:74–78. [PubMed: 8424481]

Ge X, Shea JJ. Scanning electron microscopic observation of dark cells after streptomycin perfusion of the vestibule in guinea pigs. Scanning Microsc. 1995; 9:283–288. [PubMed: 8553023]

Hashino E, Shero M. Endocytosis of aminoglycoside antibiotics in sensory hair cells. Brain Res. 1995; 704:135–140. [PubMed: 8750975]

Hashino E, Shero M, Salvi RJ. Lysosomal targeting and accumulation of aminoglycoside antibiotics in sensory hair cells. Brain Res. 1997; 777:75–85. [PubMed: 9449415]

Hayashida T, Nomura Y, Iwamori M, Nagai Y, Kurata T. Distribution of gentamicin by immunofluorescence in the guinea pig inner ear. Arch. Otorhinolaryngol. 1985; 242:257–264. [PubMed: 3907605]

Helling K, Schonfeld U, Clarke AH. Treatment of Meniere's disease by low-dosage intratympanic gentamicin application: effect on otolith function. Laryngoscope. 2007; 117:2244–2250. [PubMed: 17909448]

Hirvonen TP, Minor LB, Hullar TE, Carey JP. Effects of intratympanic gentamicin on vestibular afferents and hair cells in the chinchilla. J. Neurophysiol. 2005; 93:643–655. [PubMed: 15456806]

Ikeda M, Morgenstern C. Immunohistochemical findings of IgG recognized in the planum semilunatum of the guinea pig. J. Laryngol. Otol. 1992; 106:93–97. [PubMed: 1556500]

Imamura S, Adams JC. Distribution of gentamicin in the guinea pig inner ear after local or systemic application. J. Assoc. Res. Otolaryngol. 2003; 4:176–195. [PubMed: 12943372]

Karasawa T, Wang Q, David LL, Steyger PS. CLIMP-63 is a gentamicin-binding protein that is involved in drug-induced cytotoxicity. Cell Death Dis. 2010; 1:e102. [PubMed: 21368867]

Karasawa T, Wang Q, David LL, Steyger PS. Calreticulin binds to gentamicin and reduces drug-induced ototoxicity. Toxicol. Sci. 2011; 124:378–387. [PubMed: 21785162]

King EB, Salt AN, Eastwood HT, O'Leary SJ. Direct entry of gadolinium into the vestibule following intratympanic applications in Guinea pigs and the influence of cochlear implantation. J. Assoc. Res. Otolaryngol. 2011; 12:741–751. [PubMed: 21769689]

Kuo SW, Yang TH, Young YH. Changes in vestibular evoked myogenic potentials after Meniere attacks. Ann. Otol. Rhinol. Laryngol. 2005; 114:717–721. [PubMed: 16240936]

Lee JH, Chiba T, Marcus DC. P2×2 receptor mediates stimulation of parasensory cation absorption by cochlear outer sulcus cells and vestibular transitional cells. J. Neurosci. 2001; 21:9168–9174. [PubMed: 11717350]

Leonard RB, Kevetter GA. Molecular probes of the vestibular nerve. I. Peripheral termination patterns of calretinin, calbindin and peripherin containing fibers. Brain Res. 2002; 928:8–17. [PubMed: 11844467]

Lindeman HH. Regional differences in sensitivity of the vestibular sensory epithelia to ototoxic antibiotics. Acta Otolaryngol. 1969; 67:177–189. [PubMed: 4911527]

Liu WT, Wu JH, Li ES, Selamat ES. Emission characteristics of fluorescent labels with respect to temperature changes and subsequent effects on DNA microchip studies. Appl. Environ. Microbiol. 2005; 71:6453–6457. [PubMed: 16204579]

Lopez I, Honrubia V, Lee SC, Schoeman G, Beykirch K. Quantification of the process of hair cell loss and recovery in the chinchilla crista ampullaris after gentamicin treatment. Int. J. Dev. Neurosci. 1997; 15:447–461. [PubMed: 9263025]

Lyford-Pike S, Vogelheim C, Chu E, Della SC, Carey JP. Gentamicin is primarily localized in vestibular type I hair cells after intratympanic administration. J. Assoc. Res. Otolaryngol. 2007; 8:497–508. [PubMed: 17899270]

Lysakowski, A.; Goldberg, J. Morphophysiology of the vestibular periphery. In: Highstein, SM.; Fay, RR.; Popper, AN., editors. The Vestibular System. New York: Springer; 2004. p. 57-152.

Manzari L, Burgess AM, Curthoys IS. Dissociation between cVEMP and oVEMP responses: different vestibular origins of each VEMP? Eur. Arch. Otorhinolaryngol. 2010; 267:1487–1489. [PubMed: 20582703]

Marcotti W, van Netten SM, Kros CJ. The aminoglycoside antibiotic dihydrostreptomycin rapidly enters mouse outer hair cells through the mechano-electrical transducer channels. J. Physiol. 2005; 567:505–521. [PubMed: 15994187]

Myrdal SE, Johnson KC, Steyger PS. Cytoplasmic and intra-nuclear binding of gentamicin does not require endocytosis. Hear. Res. 2005; 204:156–169. [PubMed: 15925201]

Nicolas MT, Lesage F, Reyes R, Barhanin J, Dememes D. Localization of TREK-1, a two-pore-domain K+ channel in the peripheral vestibular system of mouse and rat. Brain Res. 2004; 1017:46–52. [PubMed: 15261098]

Oudar O, Ferrary E, Feldmann G. Ultrastructural study of the semicircular canal cells of the frog Rana esculenta. Anat. Rec. 1988; 220:328–334. [PubMed: 3259115]

Park JC, Cohen GM. Vestibular ototoxicity in the chick: effects of streptomycinon equilibrium and onampullary dark cells. Am. J. Otolaryngol. 1982; 3:117–127. [PubMed: 6979948]

Pender DJ. Gentamicin tympanoclysis: effects on the vestibular secretory cells. Am. J. Otolaryngol. 1985; 6:358–367. [PubMed: 3907388]

Plontke SK, Mynatt R, Gill RM, Borgmann S, Salt AN. Concentration gradient along the scala tympani after local application of gentamicin to the round window membrane. Laryngoscope. 2007; 117:1191–1198. [PubMed: 17603318]

Roehm P, Hoffer M, Balaban CD. Gentamicin uptake in the chinchilla inner ear. Hear. Res. 2007; 230:43–52. [PubMed: 17616288]

Salt AN, King EB, Hartsock JJ, Gill RM, O'Leary SJ. Marker entry into vestibular perilymph via the stapes following applications to the round window niche of guinea pigs. Hear. Res. 2012; 283:14–23. [PubMed: 22178981]

Sandoval R, Leiser J, Molitoris BA. Aminoglycoside antibiotics traffic to the Golgi complex in LLC-PK1 cells. J. Am. Soc. Nephrol. 1998; 9:167–174. [PubMed: 9527392]

Sandoval RM, Dunn KW, Molitoris BA. Gentamicin traffics rapidly and directly to the Golgi complex in LLC-PK(1) cells. Am. J. Physiol. Renal Physiol. 2000; 279:F884–F890. [PubMed: 11053049]

Schuknecht HF. Ablation therapy for the relief of Meniere's disease. Laryngoscope. 1956; 66:859–870. [PubMed: 13358249]

Steyger PS, Peters SL, Rehling J, Hordichok A, Dai CF. Uptake of gentamicin by bullfrog saccular hair cells in vitro. J. Assoc. Res. Otolaryngol. 2003; 4:565–578. [PubMed: 14605921]

Wang Q, Steyger PS. Trafficking of systemic fluorescent gentamicin into the cochlea and hair cells. J. Assoc. Res. Otolaryngol. 2009; 10:205–219. [PubMed: 19255807]

Wersall J, Bjorkroth B, Flock A, Lundquist PG. Sensory hair fusion in vestibular sensory cells after gentamycin exposure. A transmission and scanning electron microscope study. Arch. Klin Exp. Ohren Nasen Kehlkopfheilkd. 1971; 200:1–14. [PubMed: 5116994]

Xue J, Peterson EH. Hair bundle heights in the utricle: differences between macular locations and hair cell types. J. Neurophysiol. 2006; 95:171–186. [PubMed: 16177175]

Yoshihara T, Kaname H, Ishii T, Igarashi M. Effect of gentamycin on vestibular dark cells and melanocytes: an ultrastructural and cytochemical study. ORL J. Otorhinolaryngol. Relat. Spec. 1994; 56:24–30. [PubMed: 8121680]

Zhai F, Liu JP, Dai CF, Wang Q, Steyger PS. Evidence-based modification of intratympanic gentamicin injections in patients with intractable vertigo. Otol. Neurotol. 2010; 31:642–648. [PubMed: 20393376]
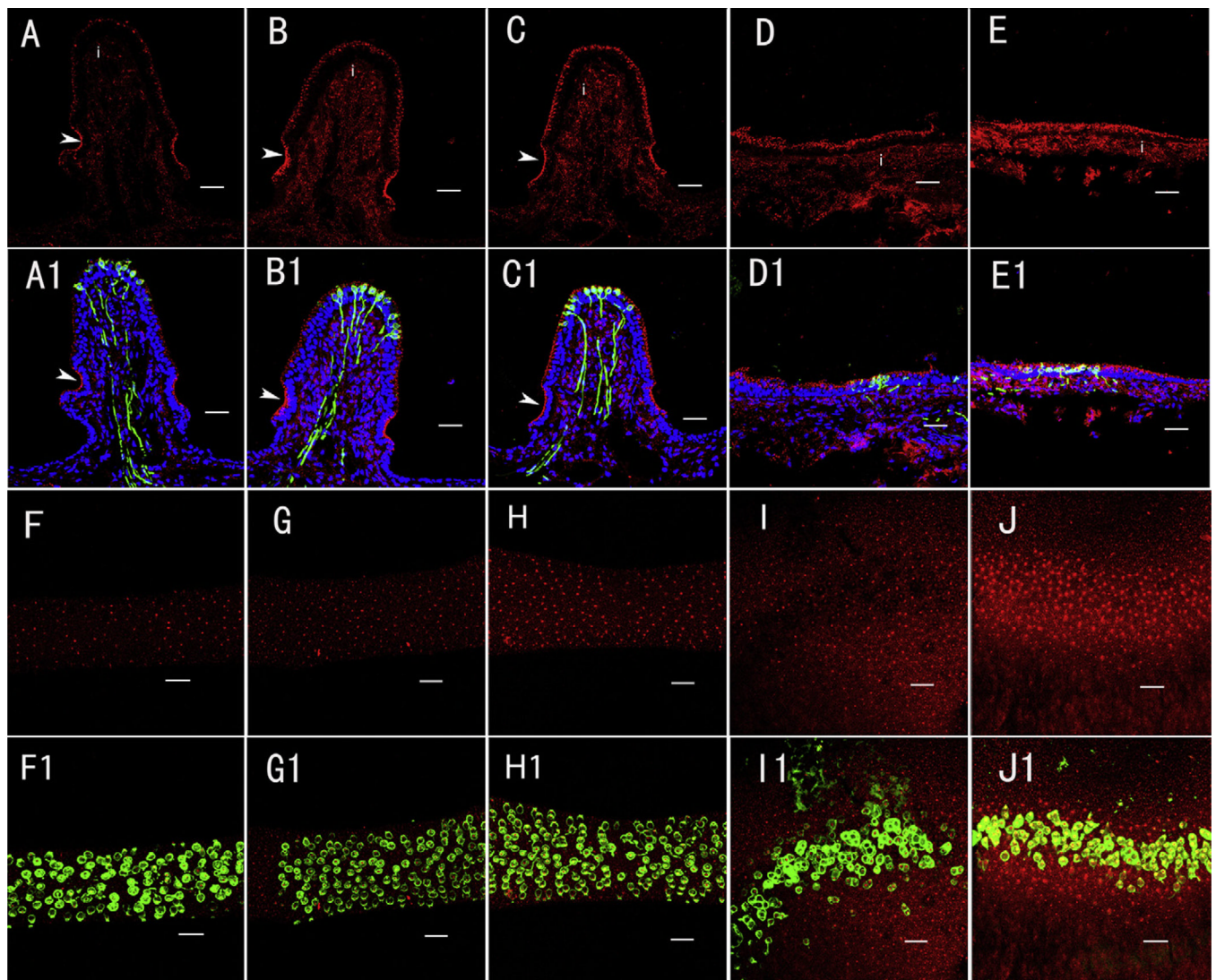
Fig. 1.
Distribution of GTTR in different vestibular organs 7 days after transtympanic administration (0.1 mg/ml GTTR in 0.05 ml). GTTR fluorescence (red) was detected in the transverse sections (A–E1) and whole-mounts (F–J1) of the superior (A, F), horizontal (B, G) and posterior (C, H) semicircular canal cristae, utricle (D, I) and saccule (E, J) respectively. A1–E1: Triple-labeled images showing GTTR (red), nuclei (blue) and calretinin immunofluorescence (green) to differentiate central zone type I hair cells from other vestibular cells in the GTTR-only panels (A–E). Blue represents DAPI labeling of ds-DNA in the nuclei of cells. Note that GTTR fluorescence within the cristae interstitial regions (i) is separated from hair cell GTTR fluorescence by a band of negligible fluorescence that corresponds with the zone occupied by supporting cell nuclei in all vestibular end-organs. Transitional cells (arrowheads) showed more intense GTTR fluorescence compared to hair cells in individual crista (A–C). F–J: GTTR fluorescence (red) in the whole-mounted superior, horizontal and posterior semicircular canal cristae, utricle and saccule respectively. F1–H1: Double-labeled images revealed intense GTTR fluorescence within the central zone hair cells (green, calretinin immunofluorescence) of individual crista in the corresponding panels (F/F1, G/G1 and H/H1). I1–J1: The striola showed more intense GTTR fluorescence than the peripheral sensory epithelia for the

maculae. Scale bar = 20 μm. (For interpretation of the references to colour in this figure legend, the reader is referred to the web version of this article.)
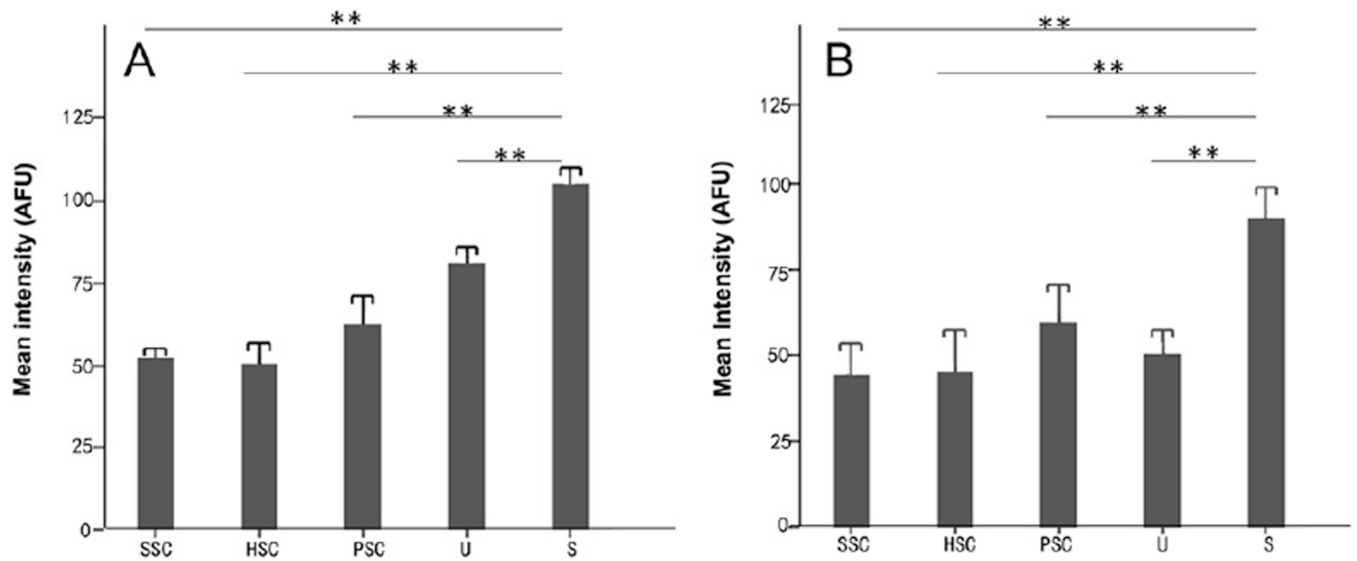
Fig. 2.
Mean intensity of GTTR fluorescence in the sensory epithelium of the five vestibular end-organs in transverse sections (A, $n = 3$ per end-organ) and from whole-mounted organs (B, $n = 3$ per end-organ) respectively. The saccule consistently had the greatest intensity of GTTR fluorescence of the 5 vestibular organs 7 days after transtympanic GTTR injection ($P < 0.001$ between saccule and any other end-organ in either group). Error bars are 1 standard deviation from the mean. SSC, superior semicircular canal; HSC, horizontal semicircular canal; PSC, posterior semicircular canal; U, utricle and S, saccule, respectively; AFU, arbitrary fluorescence units. ** represents $P < 0.001$.
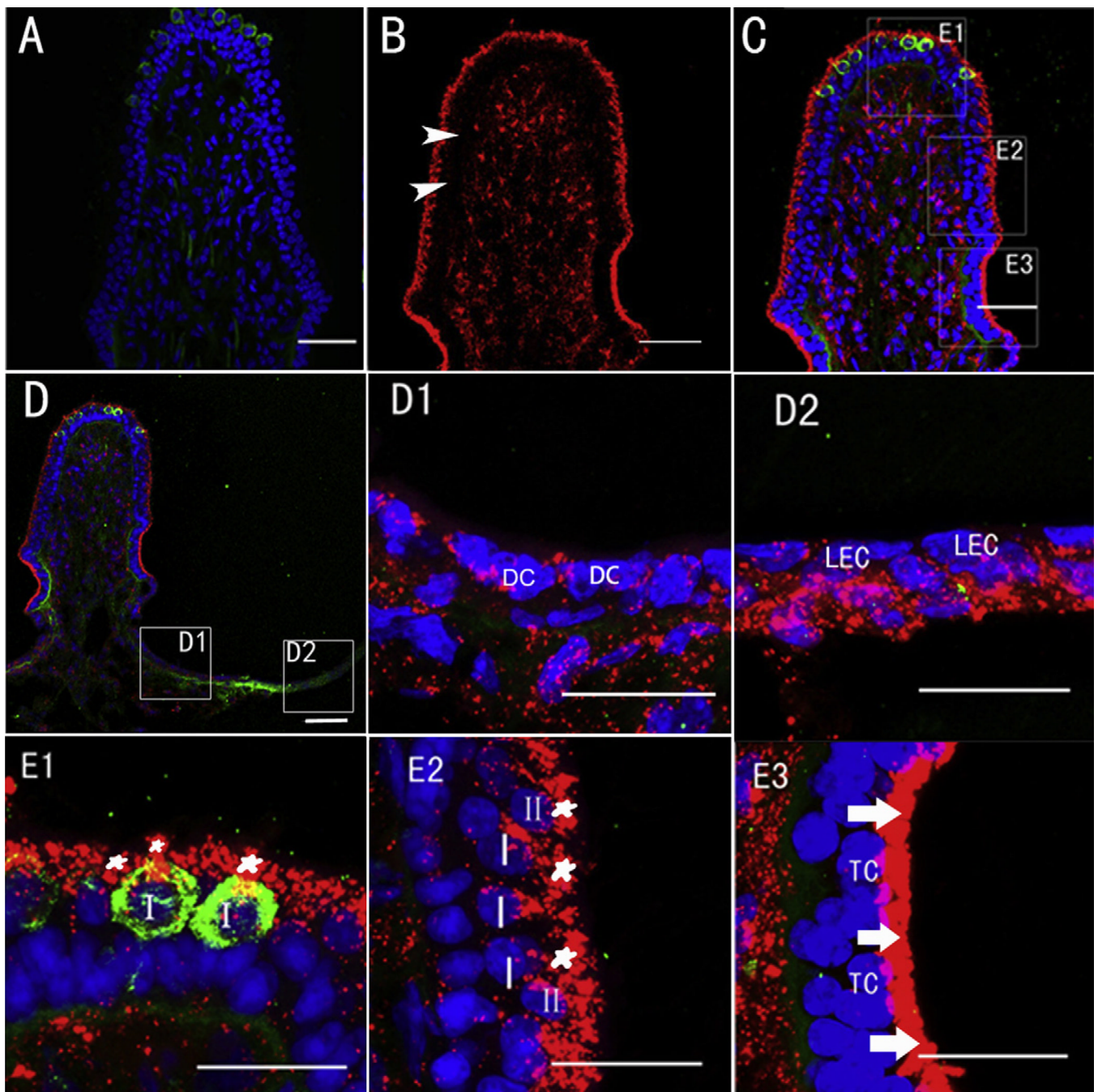
Fig. 3.
Distribution of GTTR in different cell types within the posterior crista ampullaris 7 days after transtympanic injection of GTTR (0.1 mg/ml, 0.05 ml) or TR (0.065 mg/ml, 0.05 ml). A: Negligible TR fluorescence (red) in the posterior canal 7 days after transtympanic injection of TR. B: GTTR fluorescence (red) within the cristae interstitium (i) is separated from hair cell GTTR fluorescence by a band of negligible fluorescence (arrowhead) that corresponds with the zone occupied by supporting cell nuclei in all vestibular end-organs (see C). C: Triple-labeled image of B showing positive GTTR fluorescence (red) within the central zone (E1), the peripheral zone (E2) as well as the area occupied by transitional cells (E3) in posterior canal 7 days respectively after transtympanic injection of GTTR.

Arrowhead indicates region of supporting cell nuclei that is also largely free of GTTR fluorescence (in B). D shows GTTR fluorescence in another posterior canal at lower magnification 7 days after injection. D1 and D2: Higher magnifications of the boxes shown in D with weak diffuse, and some punctate GTTR fluorescence in dark cells (DC) and lumenal epithelial cells (LEC) respectively. E1–E3 are higher magnifications of the boxes shown in C, with intense punctate GTTR fluorescence in the apical area of type I and type II hair cells (asterisk), weak punctate and diffuse labeling in most other cells, however, the most intense GTTR fluorescence occurred in transitional cells (arrow). Abbreviations: I, type I hair cell; II, type II hair cell; DC, dark cell; LEC, lumenal epithelial cell; TC, transitional cell. Blue represents DAPI labeling of ds-DNA in the nuclei of cells and green represents calretinin immunofluorescence. Scale bar = 20 μm. (For interpretation of the references to colour in this figure legend, the reader is referred to the web version of this article.)
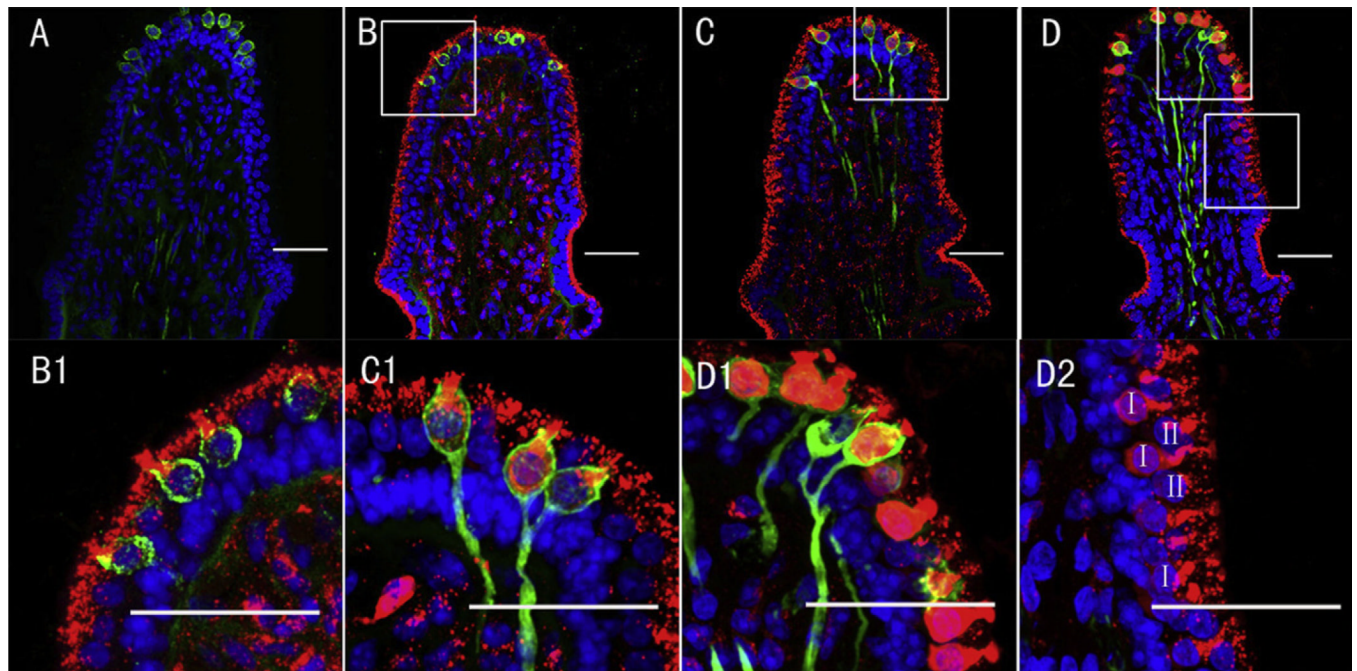
Fig. 4.
Gradient of GTTR intensity from central to peripheral type I hair cells, and beyond to type II hair cells in the crista ampullaris 7 days after transtympanic administration. A: Negligible TR fluorescence (red, if present) in posterior canal 7 days after transtympanic injection of TR. B–D show dose-dependent increased GTTR (red) intensity in hair cells at 7 days after injection of 0.1 (B, B1), 0.4 (C, C1) and 0.8 mg/ml (D, D1 and D2) GTTR. B1–D2 are higher magnifications of the boxes shown in B–D respectively. B1 (0.1 mg/ml) shows punctate GTTR mainly within the apex of type I hair cells with little diffuse fluorescence in the cytoplasm, while C1 (0.8 mg/ml) shows more GTTR fluorescence throughout the cytoplasm. D2 shows decreased GTTR fluorescence intensity in peripheral type I and type II hair cells compared to central zone type I hair cell (D1) in the crista ampullaris. Blue represents DAPI labeling of ds-DNA in the nuclei of cells and green represents calretinin immunofluorescence. I, type I hair cell; II, type II hair cell. Scale bar = 20 μm. (For interpretation of the references to colour in this figure legend, the reader is referred to the web version of this article.)
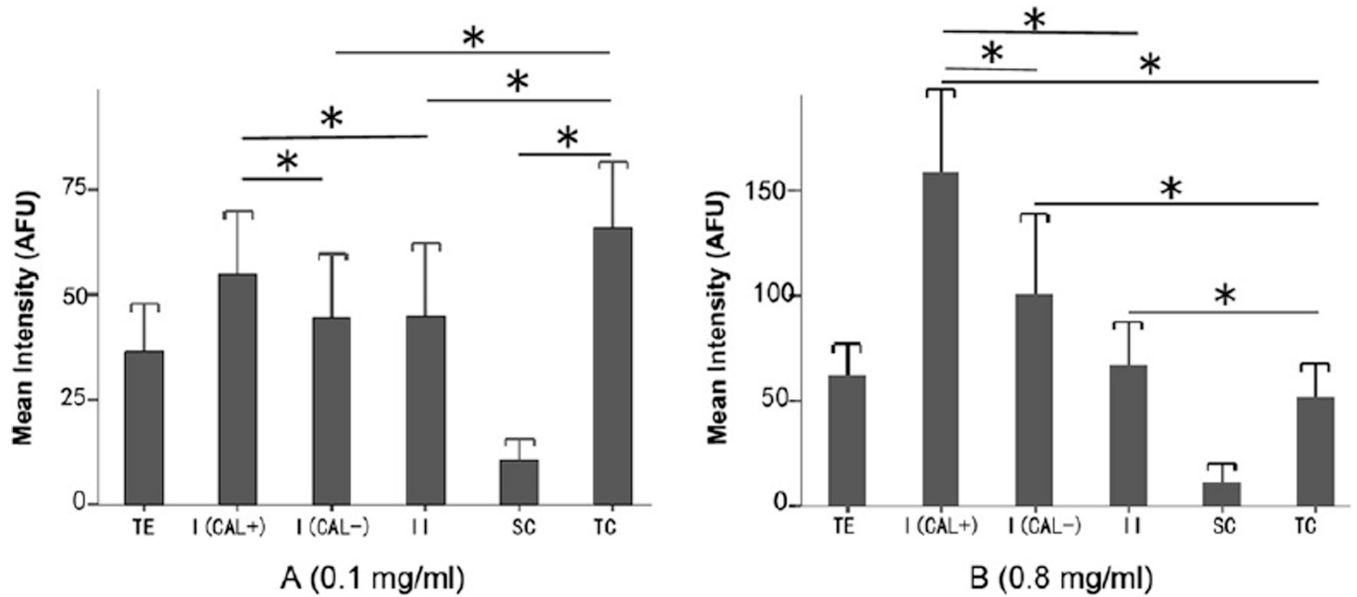
Fig. 5.
Comparison of intensity of GTTR fluorescence among different cell types of posterior crista ampularis 7 days after transtympanic administration (A: 0.1 mg/ml; B: 0.8mg/ml; $n = 4$ per end-organ). The fluorescence intensity of the whole total sensory epithelium in each transverse section was obtained by measuring all epithelial elements above the basement membrane. Intensities of GTTR fluorescence in calretinin-positive type I hair cells, calretinin-negative type I hair cells, type II hair cells, supporting cells and transitional cells were averaged and plotted in 0.1 mg (A) and 0.8 mg (B) groups respectively. More GTTR fluorescence was present in sensory epithelial regions containing central type I hair cells than peripheral type I hair cells or type II hair cells of the ampullar sensory epithelium for both 0.1 mg ($P < 0.05$) and 0.8 mg groups ($P < 0.001$). Transitional cells had more GTTR fluorescence than calretinin-negative type I ($P < 0.001$), II hair cells ($P < 0.05$), and support cells ($P < 0.001$), but not compared to calretinin-positive type I hair cells ($P = 0.297$) in 0.1 mg/ml group. In 0.8 mg/ml group, transitional cells took up less intense GTTR fluorescence than calretinin-positive and calretinin-negative type I ($P < 0.001$) and type II hair cells ($P < 0.001$). Qualitatively less GTTR fluorescence was detected in supporting cells. Error bars are 1 standard deviation from the mean. TE, total epithelium; I (CAL+), calretinin-positive type I hair cell; I (CAL–), calretinin-negative type I hair cell; II, type II hair cell; SC, supporting cell (within the sensory epithelium, below the hair cell layer); TC, transitional cell.
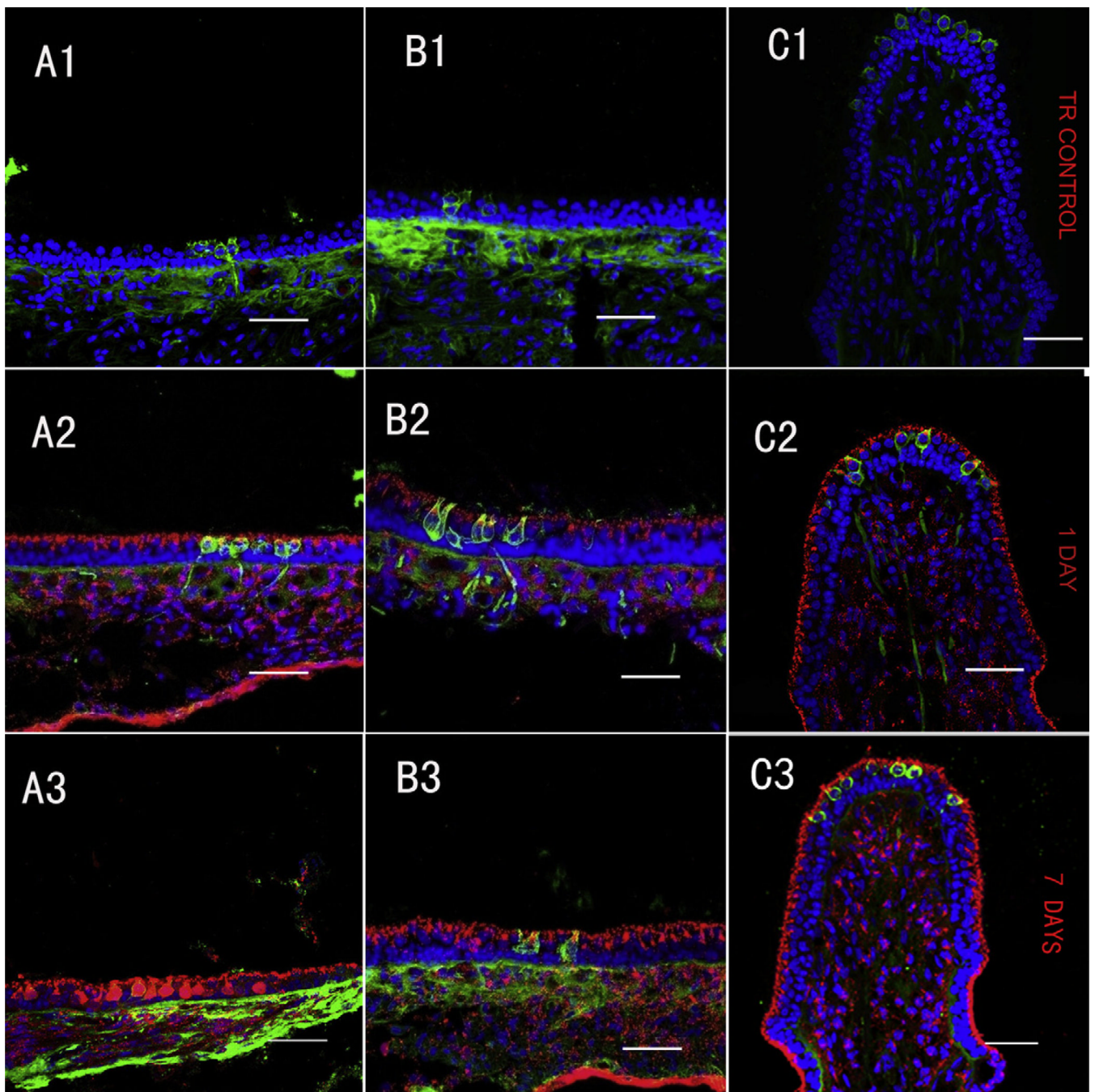
Fig. 6.
Temporal distribution of GTTR in vestibular epithelia after transtympanic administration.
A1–C1 show negligible TR fluorescence (red, if present) in the saccule, utricle and posterior
canal 7 days after transtympanic administration of TR (0.065 mg/ml, 50 µl). Transverse
sections of saccule (A2, A3), utricle (B2, B3) and posterior (C2, C3) at 1day (A2, B2, C2)
and 7 days (A3, B3, C3) labeled with GTTR (red), calretinin (green) and nuclei (blue) after a
single dose (0.1 mg/ml) transtympanic injection of GTTR. GTTR fluorescence in the
vestibular epithelia at 7 days is visibly more intense than that at 1 day after transtympanic
injection of GTTR (0.1 mg/ml, 50 µl) for each organ respectively. (For interpretation of the

references to colour in this figure legend, the reader is referred to the web version of this article.)
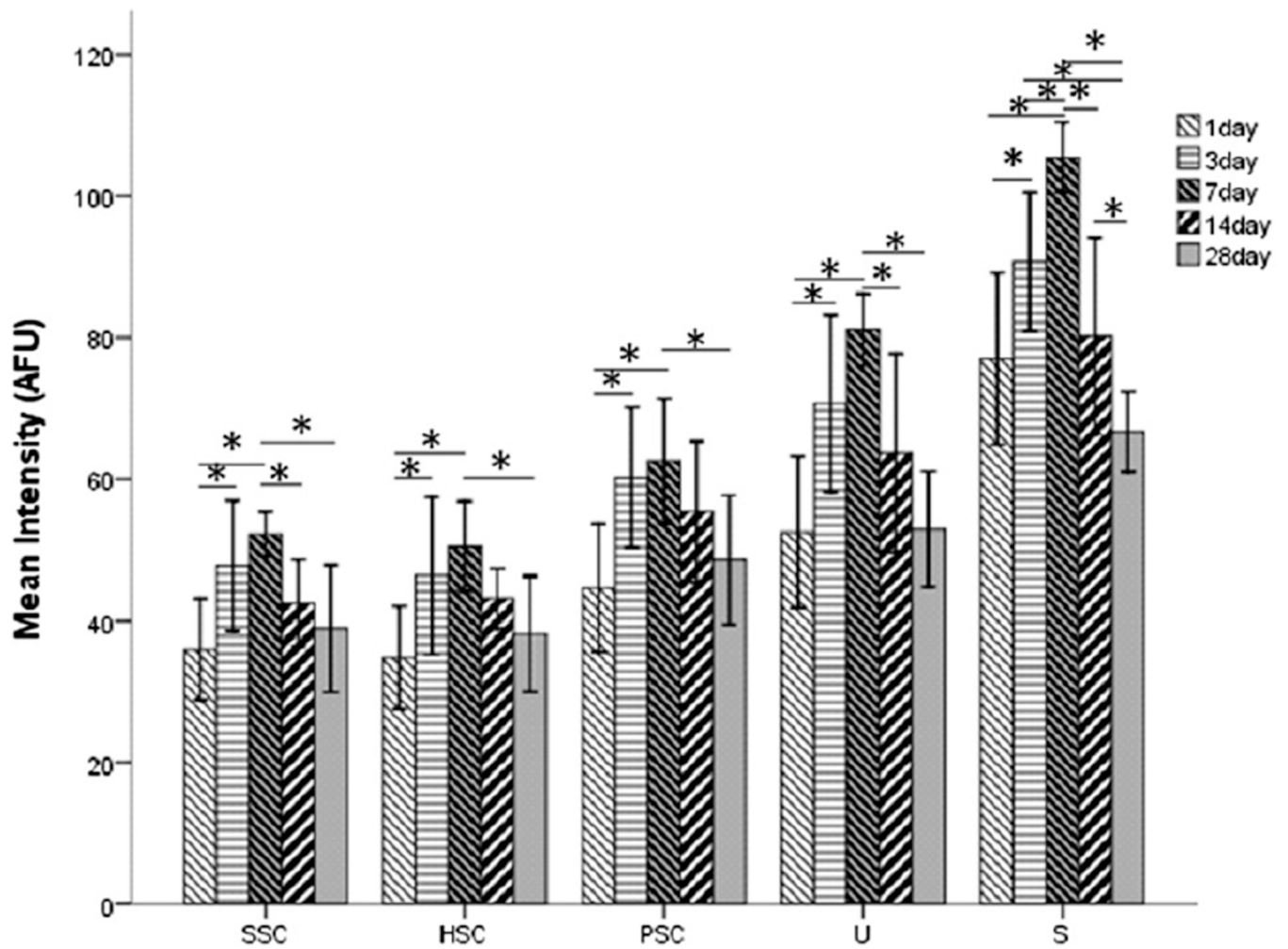
Fig. 7.
The fluorescence intensity of GTTR was measured in four mid-sections of the sensory epithelium for each end-organ and averaged as the mean intensity ($n = 4$ per end-organ). Statistically significant differences were observed between the 1 and 7 day groups, and between the 7 and 28 day groups for each vestibular organ respectively ($P < 0.05$). Error bars are 1.5 standard deviation from the mean. S, saccule; U, utricle; SSC, superior semicircular canal; HSC, horizontal semicircular canal; PSC, posterior semicircular canal.